THE PUBLISHING HOUSE
OF THE ROMANIAN ACADEMY

PROCEEDINGS OF THE ROMANIAN ACADEMY, Series A,
Volume 16, Number 2/2015, pp. 209–216

ON THE STICK-SLIP PHENOMENA IN TRACTION RAILWAY VEHICLES

Ioan SEBEŞAN[1], Ana-Maria MITU[2] , Tudor SIRETEANU[2]

[1] "Politehnica" University of Bucharest, Faculty of Transports, Bucharest, Romania
[2] Institute of Solid Mechanics of the Romanian Academy, 15 Constantin Mille St., 70701, Bucharest, Romania
Corresponding author: Ana-Maria Mitu, mitu@imsar.bu.edu.ro

The present work, regarding the stick-slip phenomena, takes into account the real shape of the friction coefficient characteristic. In the literature, this characteristic was represented by piecewise interpolation. The study in this paper is based on analytical interpolation with a single exponential function and integration of nonlinear equations of motion using the Simulink toolboxes. There are presented the conditions of stick-slip occurrence and its influence on the variables that define the motion. Moreover, there are pointed out that in the wheelset occur dynamic loads which have adverse effects on both strength and traction vehicle performance.

Key words: traction railway vehicles, adhesion force, stick-slip oscillation.

1. INTRODUCTION

When the adhesion force exceeds the drive force of motor vehicle, the wheel slips on rail causes two types of oscillations. At low slip speeds oscillations of stick-slip type occur. Their amplitude increases continuously and can reach dangerous levels and harm the system drive shaft worsening in the same time the vehicle traction performance [1–3]. At higher slip speeds, occur self vibrations which magnitude is much smaller than in the case of stick-slip. The occurrence and time development of stick-slip depend on the variation of wheel-rail friction coefficient as function of sliding speed [4–10].

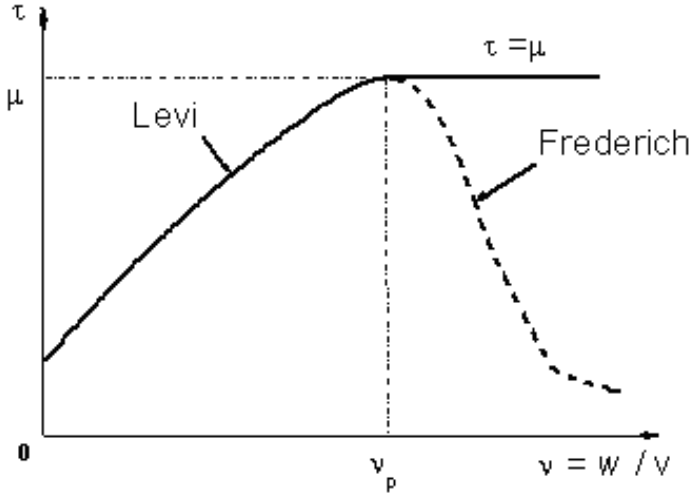

Fig. 1 – Characteristics of friction coefficient.

The friction coefficient τ depends on the rail-wheel pseudosliding ν which is the ratio between the slip velocity w and the forward speed of the wheelset v, as demonstrated by F. Carter [11].

In the Levi's law [12], the characteristic of friction coefficient has a ascending branch up to the pseudosliding value ν_p, corresponding to the maximum coefficient of friction (adhesion coefficient). As shown by Frederich F. [4], this characteristic has a descending branch for $\nu > \nu_p$ (Fig. 1).

The stick-slip oscillations occur when drive force F and friction force $T = \tau Q$ (Q being the wheel load) are decreasing characteristics function of slip velocity w, for a given value of speed ν (Fig. 2).

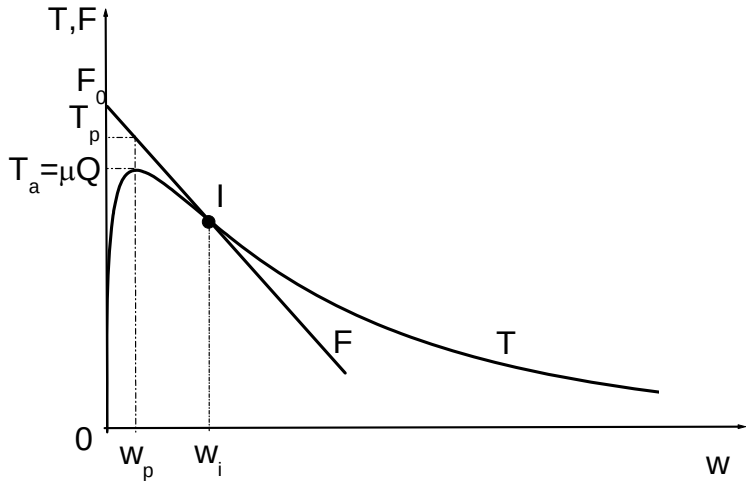

Fig. 2 – $F(\mathrm{w})$ and $T(\mathrm{w})$ characteristics for forward speed ν.

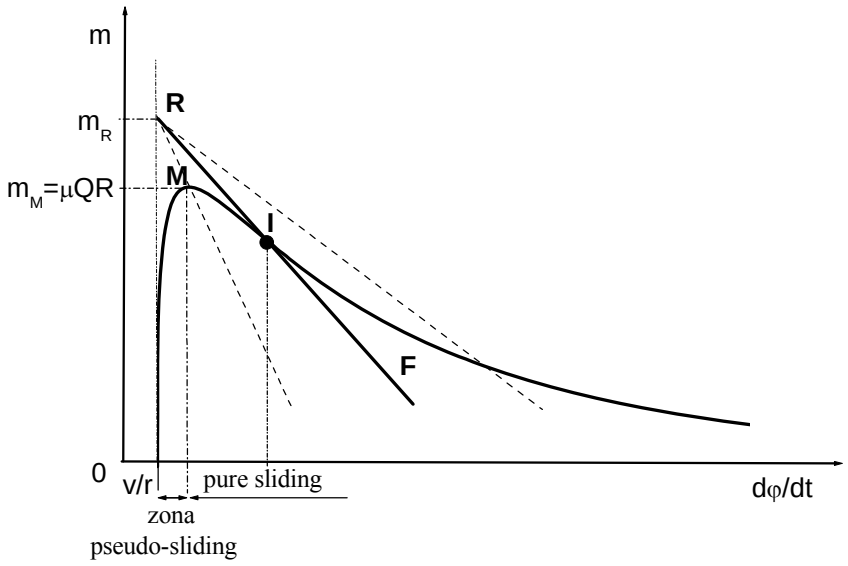

Fig. 2bis – Characteristics of torques reduced at wheels.

The tangent in I intersect vertical $\dot{\varphi} = \nu / r$ in point R. Ordinate m_R of this point defines the minimum value of torque at wheelset. Straight line RM defines the possible limit (with maximum slope) of reduced torque characteristic.

From computed data result:

$$M\left(3.24;25231\right);\ I\left(3.31;22433\right). \tag{1}$$

The equation of tangent in inflection point is:

$$m\left(\dot{\varphi}\right)=-49\ 483\dot{\varphi}+188\ 223\ \ [\text{Nm}]. \tag{2}$$

The intersection with vertical $\dot{\varphi}=\text{v}/r=3.2$ rad/s is:

$$m_{\text{R}}=m\left(3.2\right)=27\ 877\ \ [\text{Nm}]. \tag{3}$$

The slope of line RM is given by:

$$k_0=\frac{m_{\text{R}}-m_{\text{M}}}{\dot{\varphi}_{\text{R}}-\dot{\varphi}_{\text{M}}}=-66\ 150. \tag{4}$$

The equation of straight line RM is:

$$m\left(\dot{\varphi}\right)=m_R+k_0\left(\dot{\varphi}-\dot{\varphi}_R\right)=27\ 877-66\ 150\left(\dot{\varphi}-3.2\right). \tag{5}$$

This function represents the limiting characteristic of engine torque reduced at wheel. which is given by:

$$m=\frac{u}{2}m\left(\dot{\varphi}_r\right)=\frac{u}{2}\left[M_0+K_m\left(\dot{\varphi}_R-\frac{u\text{v}}{r}\right)\right]. \tag{6}$$

For $\dot{\varphi}_r=u\dot{\varphi}$ one has

$$m=\frac{u}{2}\left[M_0+K_m u\left(\dot{\varphi}-\frac{\text{v}}{r}\right)\right]. \tag{7}$$

Therefore, for $\dot{\varphi}=\text{v}/r$ it is obtained:

$$\frac{u}{2}M_0=m_R\ \Rightarrow M_0=\frac{2m_R}{u}=\frac{2\cdot 27877}{3.65}\simeq 15\ 275\ \text{Nm}, \tag{8}$$

$$\frac{u^2}{2}K_m=k_0\ \Rightarrow K_m=\frac{2k_0}{u^2}\simeq -9\ 931\ \text{Nms/rad}. \tag{9}$$

As one can observe, the point R resulted as intersection of the tangent in inflection point I with the vertical in $\dot{\varphi}=\text{v}/r$. Any line starting from a point with the ordinate less than m_R will intersect the decreasing branch characteristic of friction coefficient corresponding to the pure sliding in one or two points. If an intersection point is the portion MI of the characteristic, then appears and the second point with ordinate less than m_I. Any line, taken from a point with ordinate higher than m_R, intersects the characteristic in a single point.

Figure 3 shows an equivalent model of the driving system of engine wheelset.

The occurrence of the stick-slip phenomenon can be explained as follows: in the slip velocity range $\left(0,w_{\text{p}}\right)$, the torque of the traction motor causes torsion of its elastic shaft and of the wheelset axle. Due to the fact that at the slip velocity w_{p} the traction force $F_{\text{p}}>T_{\text{a}}$, T_{a} being the adhesion force, the wheels starts to slip with the acceleration of the drive system. At the same time there is a tension release of the elastic elements from drive system and a reduction of the forces acting on the wheel circumference up to the point I where $F=T$. Further, the motion slows down, the adhesion is restored, and in the same time the engine torque increases until it exceeds again the adhesion and the motion repeats itself [2, 3, 13].

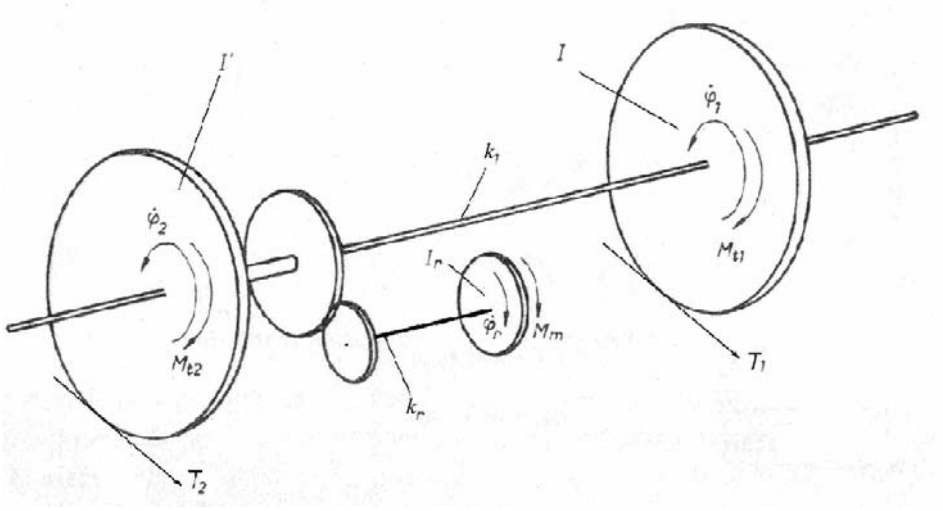

Fig. 3 – Mechanical model for stick-slip.

The system includes: the engine shaft on which acts the drive moment M_{m}, a torque shaft of the motor with stiffness k_{c}, the assembly consisting of two wheel gear with transmission ratio u, transmitting the movement from the engine shaft to the wheelset axle having stiffness k_1 and the two wheels of the vehicle on which act the moments $M_{\mathrm{t}1}, M_{\mathrm{t}2}$ of friction forces T_1, T_2: I_{r} – moment of inertia of the engine shaft; I – moment of inertia of vehicle wheel; $I' = I + u^2 I_r$ – moment of inertia of the wheel, including reduced moment of inertia of the two gear assembly drive axle , axle stiffness portion of it and the axle of the vehicle considering the infinite value u is the gear transmission ratio [6]; φ_{r} – is the angular displacement of electric engine shaft; φ_1, φ_2 – angular displacements of the vehicle wheels.

2. ANALYTICAL MODEL

As shown in Fig. 1, the analytical expression (1) provides a good approximation of Frederich's experimental relation for v = 2 m/s between the friction coefficient τ and the slip velocity w:

$$\tau(w) = 0.1 + a\left(w - b\right)^{\alpha} \exp\left(-c\, w^{\beta}\right), \tag{10}$$

where

$$\begin{aligned} &a = 1.14\left(\mathrm{m/s}\right)^{-\alpha},\ b = 10^{-5}\ \mathrm{m/s},\ c = 5.69\left(\mathrm{m/s}\right)^{-\beta} \\ &\alpha = 0.212,\ \beta = 0.811. \end{aligned} \tag{11}$$

The friction force torque is given by

$$M_{\mathrm{t}}\left(w\right) = rQ\,\tau\left(w\right), \tag{12}$$

where r is the wheel radius and Q its vertical load.

The wheel angular velocity can be expressed as function of slip velocity and forward vehicle speed as

$$\dot{\varphi} = \frac{w + \mathrm{v}}{r}. \tag{13}$$

Therefore, from (10)–(13), one can obtain the relation between friction force torque and wheel angular velocity

$$M_{\mathrm{t}}\left(\dot{\varphi}\right)=rQ\left\{0.1+a\left(r\dot{\varphi}-\mathrm{v}-b\right)^{\alpha}\exp\left[-c\left(r\dot{\varphi}-\mathrm{v}\right)^{\beta}\right]\right\}. \tag{14}$$

The variation of friction force torque versus wheel angular velocity is shown in Fig. 5.

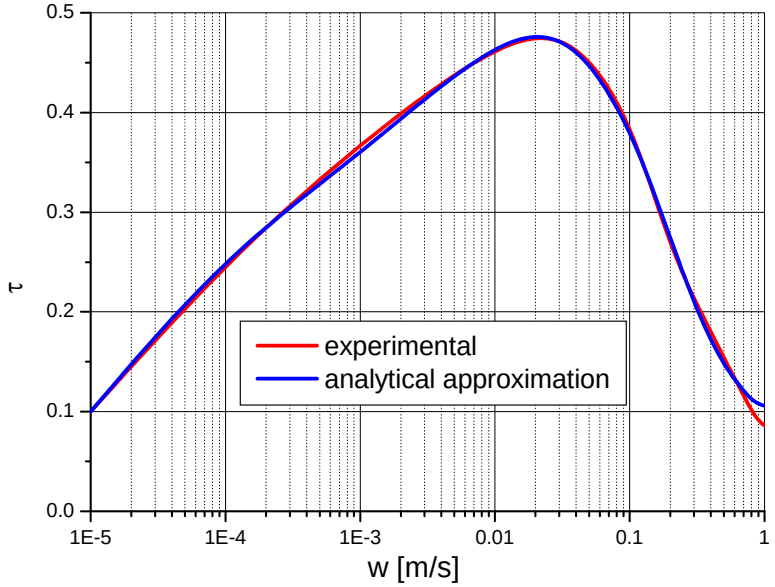

Fig. 4 – Analytical approximation of Frederich's experimental curve.

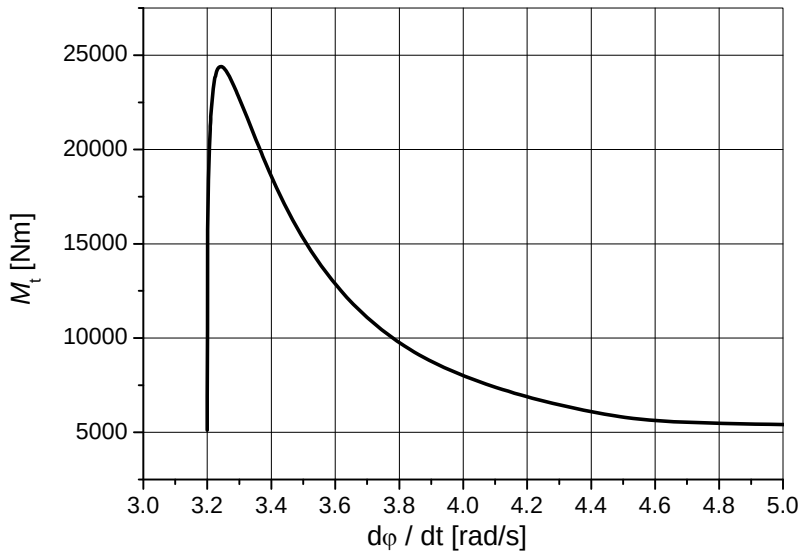

Fig. 5 – Variation of friction force torque versus angular velocity.

The equations of motion of the traction gear are (Sebesan [5])

$$\begin{aligned} &I\ddot{\varphi}_1+k_1\left(\varphi_1-\varphi_2\right)=-M_{\mathrm{t1}}\left(\dot{\varphi}_1\right)\\ &I'\ddot{\varphi}_2-k_1\left(\varphi_1-\varphi_2\right)+k_{\mathrm{r}}u\left(u\varphi_2-\varphi_{\mathrm{r}}\right)=-M_{\mathrm{t2}}\left(\dot{\varphi}_2\right)\\ &I_r\ddot{\varphi}_{\mathrm{r}}+k_r\left(\varphi_{\mathrm{r}}-u\varphi_2\right)=M_{\mathrm{m}}\left(\dot{\varphi}_{\mathrm{r}}\right). \end{aligned} \tag{15}$$

The electric engine torque $M_{\mathrm{m}}\left(\dot{\varphi}_{\mathrm{r}}\right)$ is assumed to have a linear variation of the form

$$M_{\mathrm{m}}\left(\dot{\varphi}_{\mathrm{r}}\right)=M_0+K_{\mathrm{m}}\left(\dot{\varphi}_{\mathrm{r}}-u\mathrm{v}/r\right). \tag{16}$$

For $M_{\mathrm{m}}\left(\dot{\varphi}_{\mathrm{r}}\right)$ was considered a linear variation because it was assumed that the wheelset drive is achieved with an asynchronous electric motor.

In the above relation M_0 is the torque value for the angular velocity $\dot{\varphi}_{\mathrm{r}}=u\mathrm{v}/r$ and $K_{\mathrm{m}}=\left(\dfrac{\mathrm{d}M_{\mathrm{m}}}{\mathrm{d}\dot{\varphi}_{\mathrm{r}}}\right)_{\dot{\varphi}_{\mathrm{r}}=\dot{\varphi}_{\mathrm{e}}}$, $\dot{\varphi}_{\mathrm{e}}$ being the equilibrium angular velocity.

The variation of the total friction force acting on the wheelset shaft is given by

$$T=\frac{1}{r}\left[M_1\left(\dot{\varphi}_1\right)+M_2\left(\dot{\varphi}_2\right)\right]=\frac{u}{r}\left[M_0+K_{\mathrm{m}}\left(\dot{\varphi}_{\mathrm{r}}-u\mathrm{v}/r\right)\right]. \tag{17}$$

3. NUMERICAL SIMULATION RESULTS

The system of second order differential equations (15) was integrated using Matlab-Simulink software tools. The numerical simulations were conducted for the following values of model parameters, specified by Sebesan [6]

$$\begin{gathered}Q=82\cdot10^3\,\mathrm{N},\ r=0.625\,\mathrm{m},v=2\,\mathrm{ms}^{-1},u=3.65\\ k_1=763\cdot10^4\,\mathrm{Nm}\cdot\mathrm{rad}^{-1},\ k_{\mathrm{r}}=34\cdot10^4\,\mathrm{Nm}\cdot\mathrm{rad}^{-1}\\ I=185\,\mathrm{Nms}^2\mathrm{rad}^{-1},I'=210\,\mathrm{Nms}^2\mathrm{rad}^{-1},I_{\mathrm{r}}=55\,\mathrm{Nms}^2\mathrm{rad}^{-1}.\end{gathered} \tag{18}$$

The initial conditions considered for the system of nonlinear differential equations (15) were:

$$\begin{gathered}\varphi_1\left(0\right)=\varphi_2\left(0\right)=0,\ \varphi_r\left(0\right)=0\,\mathrm{rad}\\ \dot{\varphi}_1\left(0\right)=\dot{\varphi}_2\left(0\right)=3.2\,\mathrm{rad/s},\ \dot{\varphi}_r\left(0\right)=u\mathrm{v}/r=11.68\,\mathrm{rad/s}.\end{gathered} \tag{19}$$

The numerical simulation results for $M_0=15\,300$ Nm, $K_{\mathrm{m}}=-10\,000\ \mathrm{Nm}\cdot\mathrm{srad}^{-1}$ are presented in Figs. 6–10.

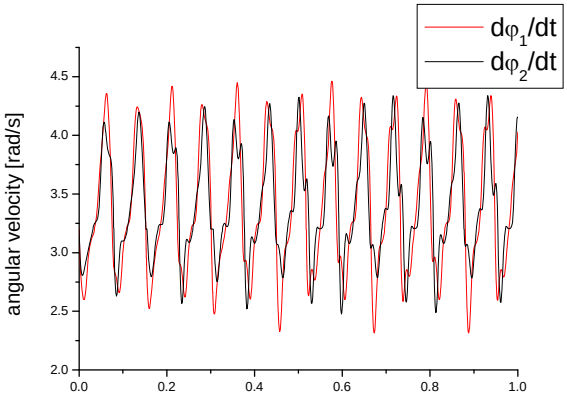

Fig. 6 – Time history of wheels angular velocity.

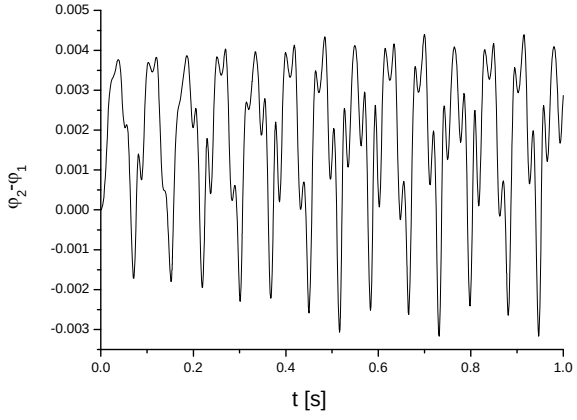

Fig. 7 – Torsion wheelset shaft during stick-slip.

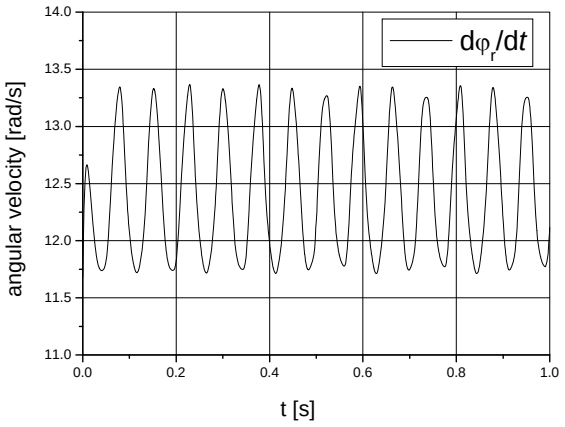

Fig. 8 – Time history of angular velocity of the traction electric engine shaft.

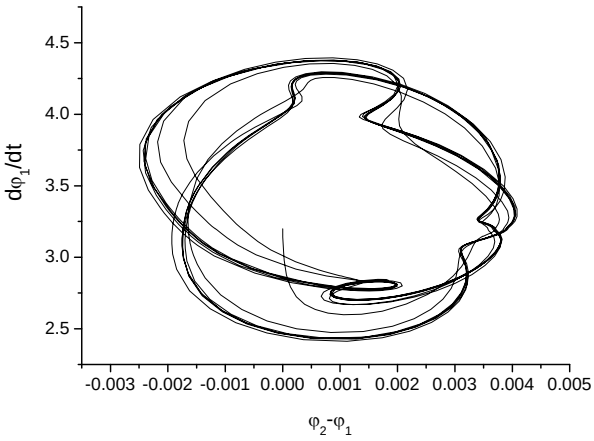

Fig. 9 – Wheel motion in phase plan $(\dot{\varphi}_1, \varphi_2 - \varphi_1)$.

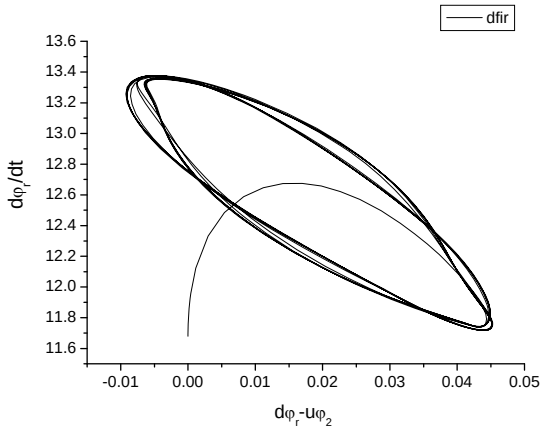

Fig. 10 – Motion of engine shaft in phase plan $(\dot{\varphi}_r, \varphi_r - u\varphi_2)$.

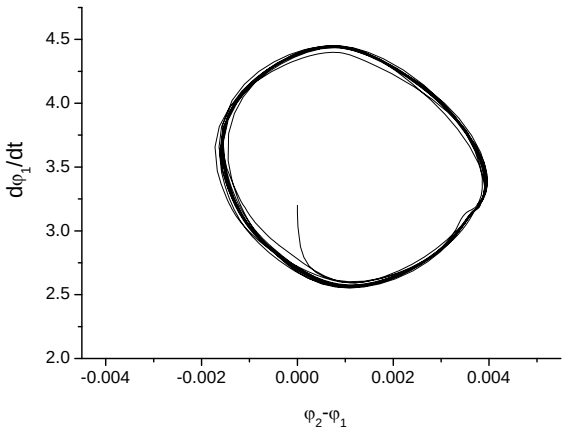

Fig. 11 – Wheel motion for $M_0 = 17\,000$ Nm.

In Fig. 6 can be observed the occurrence of stick-slip phenomenon. The "stick" can be notice at the inferior side of curves when the motion corresponds to pseudo-sliding range of friction characteristic (Fig. 5). The relative speed wheel-rail became null when the angular velocity is 3.2 rad/s. The movement will continued under this value due to the system inertia, after that the speed will increase, stick maintaining itself up to angular velocity 3.24 rad/s. At velocities $\dot{\varphi}_{1,2} > 3.2\,\text{rad/s}$ the two wheels enter the pure sliding regime, "slip" mode. In the same time occurs the decrease of the engine torque, wheels angular velocity reaching a maximum value $\approx 4.4\,\text{rad/s}$, followed by an increasing of this velocity. Torsion $\varphi_2 - \varphi_1$ of the wheelset shaft during stick-slip is shown in Figure 7. The values of the moment torque $k_1\left(\varphi_2 - \varphi_1\right)$ acting on the wheelset can harm the wheelset especially by fatigue phenomenon. During the operation was observed cracks in the wheelset shaft and even breaks if no action is taken to stop the stick-slip evolution. As one can see in Figure 8, the shaft motion is approximately harmonic, the variation of angular velocity being produced by stick-slip phenomenon. Figures 9 and 10 highlight the stability of stick-slip phenomenon. The amplitudes increase and reach extreme values corresponding to the limit cycles. With the increasing of moment M_0 one can observe faster motion stabilization. This can be explained by decreasing the influence of pseudo-sliding zone on stick-slip motion. In this case the intersection of the friction force moment characteristic with that of the engine torque occurs at higher slip velocities. For larger values of M_0 the stick-slip might not take place, the wheelset motion displaying self-vibrations as shown before.

4. CONCLUSIONS

In the paper is presented the study of stick-slip phenomenon which occurs at railway vehicles when the traction force at the wheel periphery exceeds the limited force of adhesion. The mathematical model includes the system of nonlinear differential equations characterizing the motion of the driving system of vehicle wheelset when the slip occurs in the axle. The system nonlinearity is given by the characteristic of wheel-rail friction coefficient determined from Frederich.

F. research which shows that for the micro-slip (pseudo-slip range) the theories of F. Carter, R. Levi are valid. As a result of laborious experiments, J.J. Kalker [14] has shown that the micro-slip friction coefficient at macro-slip is not maintained constant at the adhesion coefficient value, decreasing with the increasing of slip velocity.

An interpolation with a single analytical function of entire characteristic curve of friction coefficient is assessed in the paper.

A number of conclusions regarding this phenomenon are pointed out, highlighting the harmful effects of the stick-slip on the mechanical strength of driving system and on the dynamic vehicle performance. These effects can be eliminated by designing a control system of traction force at the adhesion limit. Also, the obtained results highlight the importance of taking into account the *stick-slip* phenomenon for assessing the design parameters of vehicle traction system as so to avoid the motion instability. In this way, the undesired effects of stick-slip phenomenon can be drastically reduced.

REFERENCES

1. SCHRÖTER, H., SCHÖNENBERGER, A. *Gleitworgänge zwischenRad und Schiene bei Dieseltrieb – fahrzeugen und Gegenmassnahmen durch Schrutzgeräte*, ETR, H3, 1974.
2. SEBEŞAN, I. *Die Stick-Slip-Erscheinung und seine einfluss über die dynamik der locomotiven*, Scientific Bulletin, Polytechnic Institute of Bucharest, *3–4*, 1991.
3. SEBEŞAN, I. *Dinamica vehiculelor de cale ferată*, ed. a III-a, Edit. MatrixRom, 2012.
4. FREDERICH, F., *Beitrag zur Untersuchung der Kraftschlussbeinspruchungen an schrögrollenden Schienenfahhryeugrödern.* Disertation TH Braunschweig, 1969.
5. OLTEANU, O., SEBEŞAN, I. *Mathematical model for the study of the lateral oscillations of the railway vehicle* 2012 UPB Scientific Bulletin, Series A: Applied Mathematics and Physics, **74**, *2*, pp. 105, 2012.
6. AHMADI, N., *Non-Hertzian normal and tangential loading of elastic bodies in contact*, PhD Thesis, Appendix C2, Northwestern University, Evanston I L, USA, 1982.
7. ALONSO, A., GIMENEZ, J. G. *A new method for the solution of the normal contact problem in the simulation of railway vehicles*, Vehicle System Dynamics, **43**, *2*, 2005.
8. SAUVAGE, G., PASCAL, J.P., *Nouvelle method de calcul de efforts dynamiques entres les roués et les rails. Influence du profil des roués et de l'inclinaison des rails*, Revue Générale de Chemins de Fer, sept., 1990.
9. NIELSEN, J.B., *New Developments in the Theory of Wheel/Rail Contact Mechanics*, Dissertation, TH Denmark, Lyngby, 1996.
10. MATSUMOTO, A., SATO, Y., TANIMOTO, M., QI., K., *Wheel-rail contact mechanics at full scale on the test stand*, Wear, 191, 1996.
11. CARTER, F.W., *On the action of locomotive driving wheel,* Proc. Roy. Soc. A112, 1926.
12. LEVI, R., *Étude relative au contact des roues sur rail*, Revue Géneral des Chemins de Fer, 1, 1935.
13. SEBEŞAN, I., BAIAŞU, D., *Modele mecanice in dinamica vehiculelor feroviare*, Edit. Academiei Române, Bucureşti, 2014.
14. KALKER, J.J., *Three-dimensional elastic bodies in rolling contact*, Kluwer Academic Publishers, Dortrech E.A., 1990.

Received January 26, 2015